

<sup>1</sup> Institute for Soil, Climate and Water of the Agricultural Research Council (ARC-ISCW), Stellenbosch, South Africa

<sup>2</sup> Climat et Occupation du Sol par TELedetection (COSTEL), UMR 6554/LETG-CNRS, University of Rennes-2, Rennes, France

<sup>3</sup> Laboratoire de Météorologie Physique (LaMP), UMR 6016-CNRS, Blaise Pascal University, France

## Sea breeze development under an offshore synoptic wind in the South-Western Cape and implications for the Stellenbosch wine-producing area

V. Bonnardot<sup>1</sup>, O. Planchon<sup>2</sup>, and S. Cautenet<sup>3</sup>

With 11 Figures

Received May 26, 2003; revised July 29, 2004; accepted August 4, 2004

Published online February 22, 2005 © Springer-Verlag 2005

### Summary

Sea breezes were investigated during the maturation period of wine grapes in the South-Western Cape under particular synoptic wind conditions (onshore for Table Bay and offshore for False Bay). Observations from an automatic weather station network located in the Stellenbosch wine-producing area as well as the Regional Atmospheric Modelling System (RAMS, non-hydrostatic, parallel, version 4.3) were used. Results showed that two sea breezes developed, one from Table Bay late in the morning, and the other from False Bay later in the afternoon. The coastal low strengthened and deflected the sea breeze from Table Bay towards the south and south-east of the study area, while the offshore large-scale circulation hindered the development of the sea breeze in the opposite direction over False Bay and delayed its movement towards land. The decrease in temperature resulting from the onset of the sea breeze from the Atlantic early in the afternoon could be significant for viticulture, reducing the duration and intensity of high temperature stress on grapevine functioning at the coolest locations.

### 1. Introduction

Sea breezes have been studied extensively in many regions of the world in the past, firstly by means of surface and upper air observations, then

by means of early linear analytical models and, more recently, by means of complex non-hydrostatic numerical models. Abbs and Physick (1992) presented a well-documented overview of these studies to show the characteristics of the sea breeze, its behaviour in complex terrain and its ability to penetrate hundreds of kilometres inland. Characteristics of the sea breeze in South Africa have not been extensively documented, with the notable exceptions being the KwaZulu-Natal coast along the Indian Ocean (Jackson, 1954; Preston-Whyte, 1969) and the West Coast of Namibia (Jackson, 1954; Tyson and Seely, 1980; Lindesay and Tyson, 1990). The lack of knowledge concerning this phenomenon on the South African west and south-west coast gives us reason to investigate the sea breeze in the extreme South-Western Cape, particularly because of its unique location (Fig. 1). The South-Western Cape is flanked by the Atlantic Ocean, with the cold Benguela current to the west and the warmer Agulhas current to the south generating significant sea surface temperature differences between Table Bay to the west and

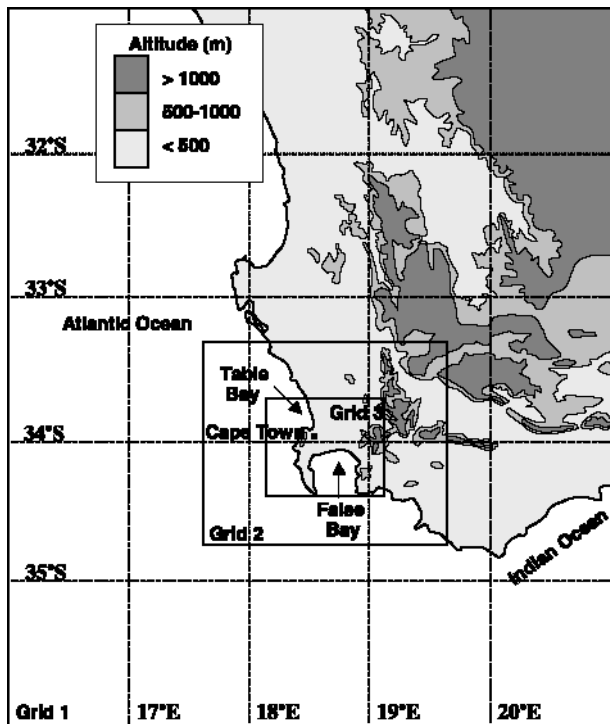


Fig. 1. Study area and three nested grids for simulations over the extreme South-Western Cape of South Africa

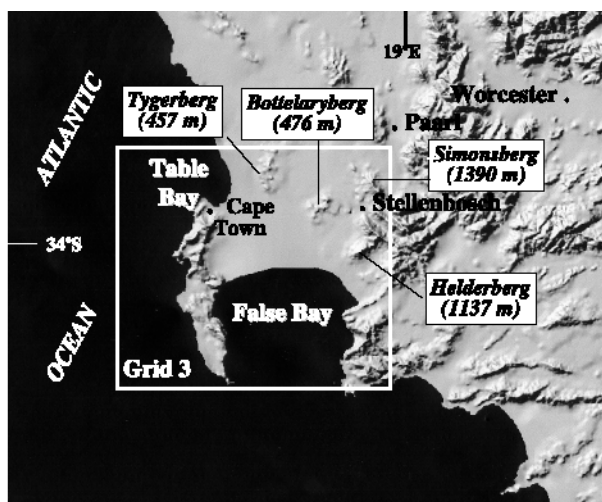
False Bay to the south. It is possible for two bay breezes (from Table Bay and False Bay), or an ocean breeze (from the Atlantic) and a bay breeze (from False Bay), to develop and converge, as observed by Physick and Abbs (1991) in Australia. The complex coastlines associated with a mountainous inland terrain with relatively high ranges (Helderberg and Simonsberg at 1100–1400 m), valleys and plains (Fig. 2a) result in local circulations so that up- and down-slope breezes could develop and act together with the sea breeze, as shown by Mahrer and Pielke (1977).

The meso-scale climatic implications of the sea breeze in one of the most famous South African wine-producing areas provided further impetus for sea breeze investigations in this region (Fig. 2b). The associated increase in wind velocity in the afternoon and concomitant increase in relative humidity and reduction in temperature is of particular interest for the wine industry due to the significant effects of temperature (Kliewer and Torres, 1972; Coombe, 1987), relative humidity (Düring, 1976; Champagnol, 1984; Gladstones, 1992) and wind (Freeman et al., 1982; Campbell-Clause, 1988; Hamilton, 1989) on grapevine functioning and thus poten-

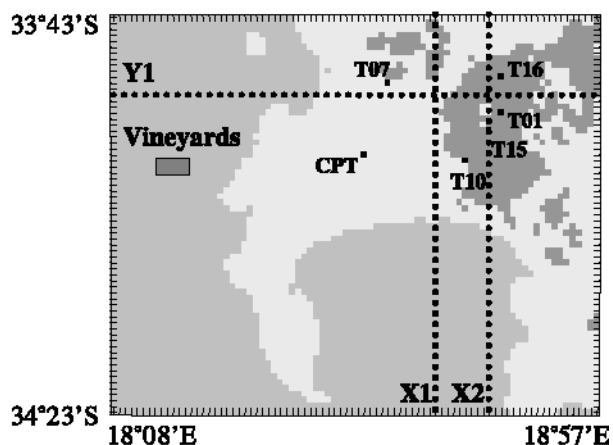
tially on wine character and quality. The interactions between climatic parameters and grape performance and wine quality and character have been previously compiled (Champagnol, 1984; Huglin and Schneider, 1998) and summarized (Carey et al., 2002).

Sea breeze studies were initiated using surface data from the ARC-Infruitec/Nietvoorbij automatic weather station network situated in the vineyards of the Stellenbosch and Drakenstein districts for the month of February over three years (1996, 1997 and 1998). These data were collected in order to investigate the inland penetration and climatic influences of the sea breeze in the wine region during the ripening period of most cultivars in the Cape (Bonnardot, 1997, 1999). The frequency analysis of the surface winds revealed that 30 to 64% of the wind directions, depending on the locations, were of sea origin, especially in the afternoon. There was also a sudden change in direction from predominantly north and north-east (land origin) at night to predominantly west and south-west (sea origin) in the afternoon, accompanied by an increase in wind velocity (mean maximum wind velocity of  $5 \text{ m s}^{-1}$  at 17:00).

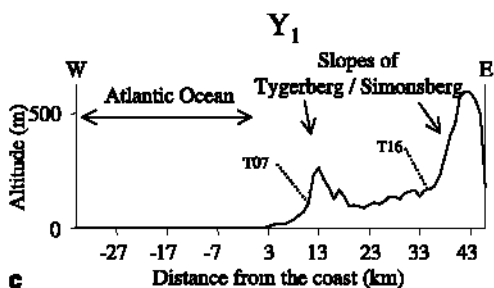
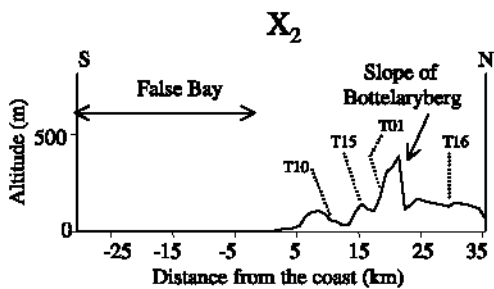
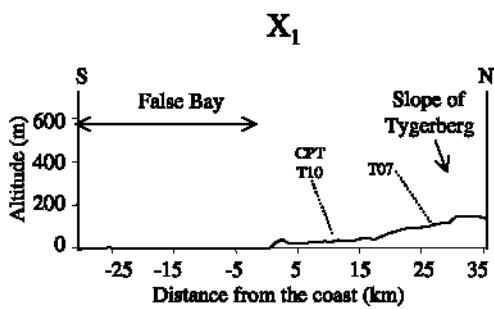
Modelling methods soon appeared necessary in order to study the atmospheric profiles, the origin of the sea breeze and its characteristics in more detail. Preliminary numerical simulations were performed over the Stellenbosch-Drakenstein wine-producing area using two nested grids (25 km and 5 km resolution) for days when the synoptic wind was onshore (Planchon et al., 2000; Bonnardot et al., 2001). At the maximum stage of the sea breeze development (17:00 South African Standard Time-SAST), the modelled results for the 5 km grid resolution showed that the penetration of the sea breeze resulted in cooler temperatures ( $< 25^\circ\text{C}$ ) closer to the coast and that the optimum temperature requirements for grapevine photosynthesis ( $25\text{--}30^\circ\text{C}$  in Kriedemann, 1977) were met in a region located between approximately 15 and 35 km from False Bay, results which are similar to the observations in the vineyards. In order to ascertain the contributing effects of topography to the local circulation, further simulations were performed using a third grid and a 1 km resolution (Bonnardot et al., 2002). Temperature differences between the south-facing and north-facing slopes



a



b



c

Fig. 2. a) Model area (grids 2 & 3) (Geographical data – University of Stellenbosch); b) Location of the vineyards and automatic weather stations within Grid 3 (CPT = Cape Town International Airport); c) Cross sections at 18°41'E (X<sub>1</sub>), 18°47'E (X<sub>2</sub>) and 33°47'S (Y<sub>1</sub>) over the Stellenbosch wine-producing area

near the coast were significant, with potential implications for viticulture. A prevailing southern synoptic wind, as used in the above simulations, however, is not the only wind direction that occurs during the maturation period. A frequency

analysis of the 850 hPa winds at Cape Town International Airport between 12:00 and 13:00 SAST for February 1995–2000 (Maritz, 2001) showed that 66% of the recorded winds had a westerly or southerly component (sea origin)

and 30% had a northerly or easterly component (land origin). Since the percentage of winds originating over land is significant over the extreme South-Western Cape, it was also relevant to study and present climatic observations in the vineyards and results of numerical simulations for a very hot day associated with “Berg wind” conditions (South African name for mountain wind).

## 2. Data and method

The three-dimensional Regional Atmospheric Modelling System (RAMS, non-hydrostatic, parallel, version 4.3) developed at the Colorado State University (Pielke et al., 1992; Cotton et al., 2003) was used to run the numerical simulations. Simulations were performed at the *Laboratoire de Météorologie Physique* (LaMP) of the Blaise Pascal University in Clermont-Ferrand in co-operation with the laboratory “Climat et Occupation du Sol par TELétection” (COSTEL) of the University of Rennes-2, both CNRS units in France. The numerical model RAMS is based on the basic physical equations which govern the processes operating in the atmosphere. RAMS uses nested grids to cover a large domain at low resolution and simulate the large-scale circulation, while providing higher spatial resolutions. Three nested grids (25 km, 5 km and 1 km) were used within the South-Western Cape (Fig. 1 and Table 1). The finer resolution grid communicates with its coarser-resolution parent grid via two-way interaction following the scheme designed by Clark and Farley (1984) and Walko et al. (1995).

The atmospheric model takes meteorological fields as well as sea surface temperature (SST), topography, vegetation and soil data into account as initial fields in order to adjust the model state towards observations. A global gridded dataset of meteorological fields produced by the European

Centre for Medium-range Weather Forecasting (ECMWF), including humidity, wind speed and direction, air pressure and temperature on a number of air pressure levels (every six hours at 30 levels up to 9000 m), was used both as initial fields and as time-dependant fields to which the lateral boundaries of Grid 1 was nudged during integration, but with no nudging in the centre of the model. A time step of 10 seconds and 35 levels in the vertical dimension (same in both grids) with 15 levels from surface to 1500 m (ensuring a fine description of the boundary layer) was used. The vertical grid spacing was 30 m near the ground with a geometric stretch ratio of 1.2 and a maximum interval of 1000 m above 3000 m up to the model top (9000 m). Local sea surface temperatures (SST) measured along the coast of the South-Western Cape and supplied by the South African Weather Service (SAWS) were added to those obtained from the ECMWF derived from Meteosat satellite in order to take into account the large variation in local SST. They were held constant in time during the run. Topographical data were obtained from NOAA (resolution 1') and the land use data were provided by the ARC-ISCW. The land use data file is a 200-m grid resolution, which was aggregated to the lower resolutions and adjusted to the 30 land cover classes used by RAMS. These classes are mostly characterized by vegetation type or whether the surface is covered with water, bare-ground or urban. Each of these classes is assigned a set of land surface parameter values including leaf area index, vegetation fractional coverage, vegetation height, albedo and root depth. A total of 12 soil texture classes are also parameterised in RAMS, but in this specific study it was assumed that the soil was homogeneous and the soil class used was sandy loam due to the high frequency of this type of soil in the vineyards (Land type survey staff, 1995). Soil

**Table 1.** Description of nested grids for meso-scale atmospheric numerical simulations with the Regional Atmospheric Modelling System (RAMS)

	Grid point resolution (km)	Latitude	Longitude	Dimensions (km)	No of grid points
Grid 1	25	31°00'S–36°00'S	16°00'–21°00'E	550 × 475	418
Grid 2	5	33°15'S–34°45'S	17°40'–19°30'E	160 × 160	1024
Grid 3	1	33°43'S–34°23'S	18°08'–18°57'E	67 × 82	5494

**Table 2.** Attributes of the five automatic weather stations used and located in the Stellenbosch wine-producing area

Location	Altitude (m)	Aspect	Slope (%)	Distance from West Coast (km)	Distance from False Bay (km)
T01	148	SSW	1.68	35	20
T07	230	SE	8.62	12	27
T10	130	SW	5.73	24	12
T15	150	S	9.59	28	16
T16	260	NE	7.49	35	30

moisture was obtained from ECMWF. As the file was not homogeneous, it was assigned according to soil texture.

The run started at 00:00 UTC on 18/02/2000 and finished at 24:00 UTC the following day. Meteorological fields of wind, temperature and relative humidity were studied. Results for 08:00, 14:00 and 17:00 South African Standard Time (SAST) on 18/02/2000 are presented using horizontal cross sections within the domain covered by the two coarser grids (Fig. 1), and horizontal and vertical cross sections within the domain covered by Grid 3 (Fig. 2). Surface meteorological data (hourly temperature, relative humidity, wind speed and direction) from the ARC Infruitec-Nietvoorbij automatic weather station network, located in the vicinity of a vineyard, were analyzed to show the climatic patterns in the vineyards around Stellenbosch (Fig. 2b). Characteristics of their locations are given in Table 2. Their approximate location is also shown along the cross-sections (Fig. 2c).

Because the agro-climatic automatic weather stations are not always representative of their locality and their measurements are subject to microclimatic peculiarities in the immediate vicinity of the station (Oke, 1978; White et al.,

1992), upper air data (measured from an air balloon) and surface data from Cape Town International Airport (SAWS, 2000) were also used to verify the outputs of the atmospheric model. Time is given as South African Standard Time (SAST), i.e. Greenwich Meridian Time +02:00, unless otherwise specified.

### 3. Results and discussion

#### 3.1 Meteorological conditions on 18 February 2000

When a strong high-pressure system exists over the interior of the south-west of South Africa, and a low-pressure system (coastal low) is situated along the West Coast of South Africa, it produces warm offshore airflow (berg winds) ahead of the system and cooler onshore airflow behind it, as it moves towards the south and the south-east (Fig. 3a).

The continental high pressure and the coastal low were clearly identified on the synoptic weather map for the 18 February 2000 (Fig. 3b, SAWS, 2000). The Atlantic Ocean High (AOH) was situated to the south-west of Southern Africa and the Western Cape was partly cloudy

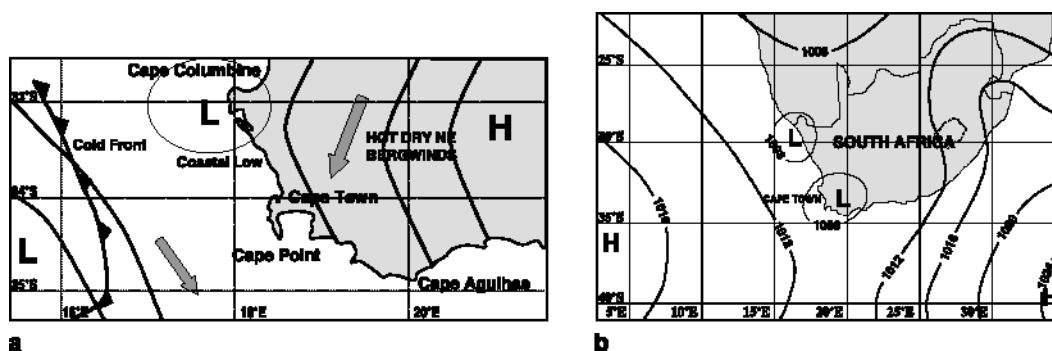


**Fig. 3.** a) Sea-level chart diagram over the Western Cape and b) Synoptic chart for 18 February 2000 at 12:00 UTC – 14:00 SAST (adapted from SAWS, 2000)

with northerly winds over the interior and easterly winds along the South Coast. Very hot and dry conditions were recorded over the region. At night, the north-easterly to north-westerly winds brought in a hot and dry air layer, 24 to 28 °C and 15 to 20% relative humidity between 1000 and 1500 m, the corresponding 900 and 850 hPa air pressure levels, while the surface north-easterly wind was weak (3 m s<sup>-1</sup>) with cool (18.5 °C) and humid (70% relative humidity) conditions (Fig. 4a). In the afternoon (12:38), the northerly wind strengthened (above 10 m s<sup>-1</sup>) from

900 hPa upwards and was associated with warm (24–25 °C) and dry (30% relative humidity) conditions, while the surface wind was north-west (onshore), also strong (above 10 m s<sup>-1</sup>) with warm (26 °C) and dry (40% relative humidity) conditions (Fig. 4b). Moreover, surface data from Cape Town International Airport showed that relative humidity was 47% at 14:00 SAST, but the maximum temperature for the day reached 37.4 °C at 11:00 SAST, which was 11.4 °C above the mean February maximum temperature (mean 1961–1990). Knowing that vines require

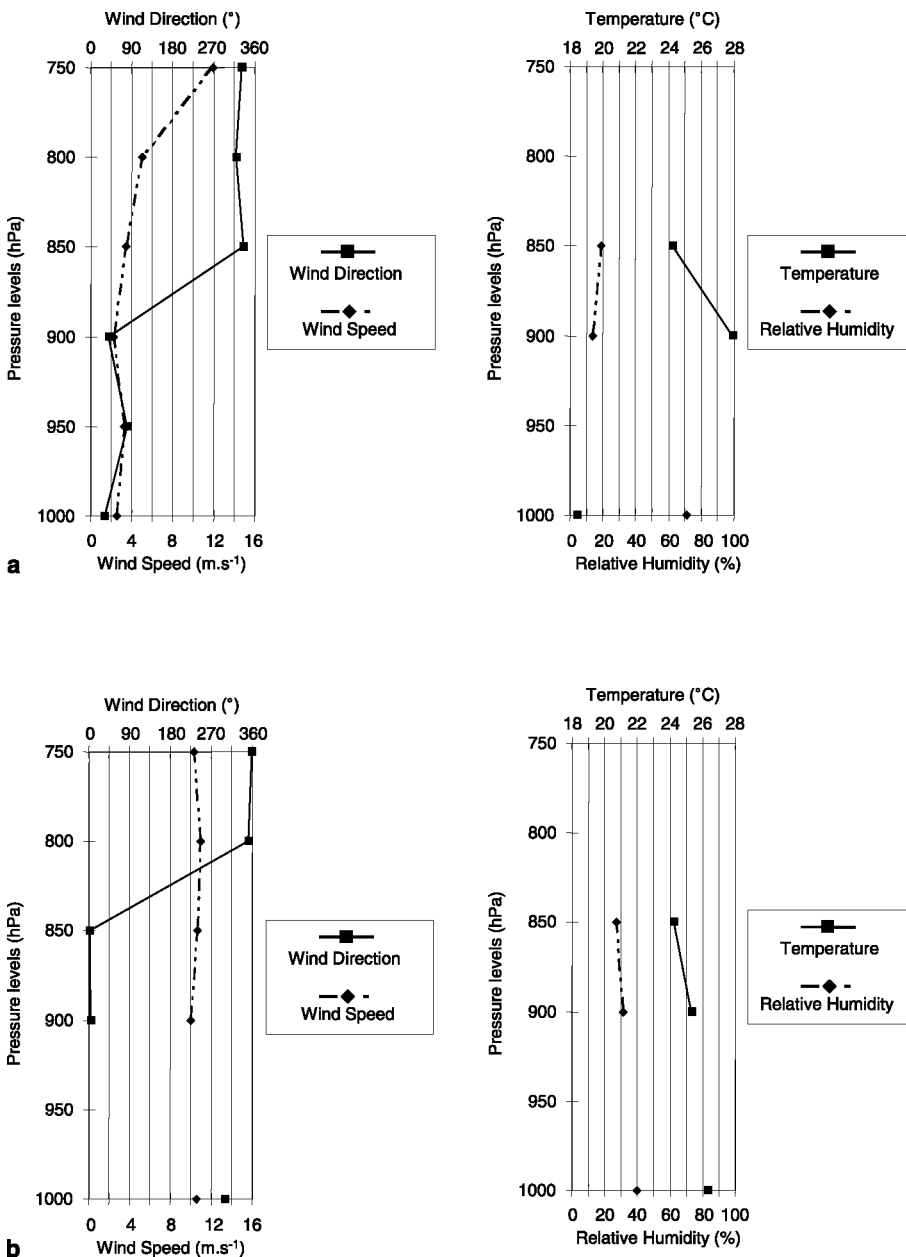


**Fig. 4.** Surface and upper air data at Cape Town International Airport at different air-pressure levels. Wind direction and wind speed (left); temperature and relative humidity (right) on 18 February 2000 at **a)** 01:25 and **b)** 12:30 (SAST). Source: South African Weather Service

a temperature of 25 to 30 °C (Kriedemann, 1977), a relative humidity of 60 to 70% (Champagnol, 1984) and a wind below 4 m s<sup>-1</sup> (Campbell-Clause, 1988) for maximum photosynthetic activity, these hot, dry and windy conditions generated a period of stress for the grapevine.

Sea surface temperatures were cold on the Atlantic side near Cape Town due to the Benguela current and coastal upwelling, 11 °C at Koeberg and Sea Point, and warmer (between 19° and 22 °C) in False Bay, resulting in significant temperature differences between sea and land and enabling the development of a sea breeze.

### 3.2 Climatic observations in the vineyards and indications of a sea breeze presence

Surface data in the vineyards showed a change in wind direction from predominantly north, north-east and east (land origin) at night until 11:00 to 12:00 SAST, to progressively north-west until 16:00 SAST, then west until 19:00 SAST and finally west to south in the evening (Fig. 5a). All afternoon wind directions are of sea origin considering the location of the weather stations. This change in direction was accompanied by an increase in wind velocity in the afternoon

(Fig. 5b). The north westerly and westerly winds strengthened from 10:00 SAST onwards (maximum wind speed recorded from 11:00 to 13:00 SAST) and reached a velocity of 4 to 8 m s<sup>-1</sup> depending on the locations, i.e. above the recognized 4 m s<sup>-1</sup> threshold that results in increased stomatal resistance (Campbell-Clause, 1988). This wind speed was similar to that recorded during sea breeze circulations in temperate latitudes, which is usually between 4 and 6 m s<sup>-1</sup> (Janoueix-Yacono, 1995).

The air dried as the land warmed. The minimum relative humidity was recorded at 12:00 SAST at stations closest to Table Bay (T07) or False Bay (T10), and 13:00 SAST at stations located between 15 and 30 km from False Bay, or between 28 and 35 km from Table Bay (T15, T01 and T16). Even though relative humidity values remained low (between 20 and 65% depending on the location), a slight humidity increase (ca. 10%) was recorded at stations close to the sea between 12:00 and 13:00 SAST for T10 and T07, an hour later, between 13:00 and 14:00 SAST for T15, T01 and T16 and remained constant until 15:00 SAST (Fig. 5c). The humidity dropped slightly at 15:00 SAST (a second minimum was recorded at 16:00 SAST) and increased again from 16:00 SAST onwards.

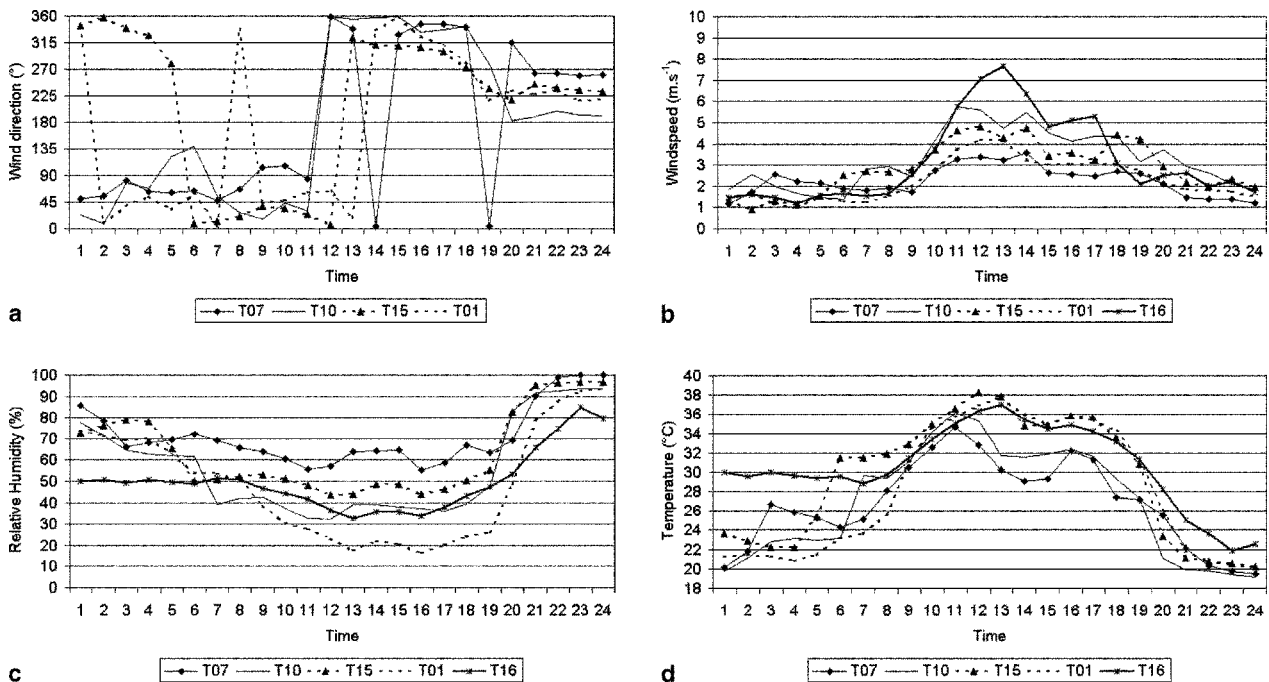


**Fig. 5.** Hourly **a)** wind direction (°), **b)** wind speed (m s<sup>-1</sup>), **c)** relative humidity (%), **d)** temperature (°C) observed in the Stellenbosch wine-producing area on 18 February 2000

Despite warm conditions (maximum temperature above  $30^{\circ}\text{C}$  in the vineyards), both humidity increases corresponded to temperature decreases, which were less significant with distance from the shoreline. Two groups of stations could be distinguished from the temperature patterns:

- T07 (12 km from Table Bay) and T10 (10 km from False Bay) recorded an early maximum temperature at 11:00 SAST. The temperature dropped from  $34\text{--}36^{\circ}\text{C}$  to  $30\text{--}32^{\circ}\text{C}$  respectively, between 11:00 and 13:00 SAST with a minimum of  $28\text{--}32^{\circ}\text{C}$  at 14:00 SAST (the usual time recorded for maximum temperature), which is a temperature decrease of  $6^{\circ}\text{C}$  in 3 hours (Fig. 5d). As a result, the duration and intensity of thermal stress for grapevine functioning could have been reduced.

- T15, T01 and T16, located at 16, 20 and 30 km from False Bay respectively, recorded their maximum temperature an hour (T15) or two (T01, T16) later (at 12:00 and 13:00 SAST respectively) than T07 and T10. The temperature decrease was not as significant (only  $3^{\circ}\text{C}$ ) as for the previously mentioned stations and the region was still subject to warm conditions, which may have stressed the vine.

### 3.3 Results of simulations and discussion

*Synoptic conditions:* At 08:00 SAST, the modelled upper winds had a northerly component, especially those to the north of the study domain (Fig. 6a). These probably correspond to the winds to the west of the high-pressure system

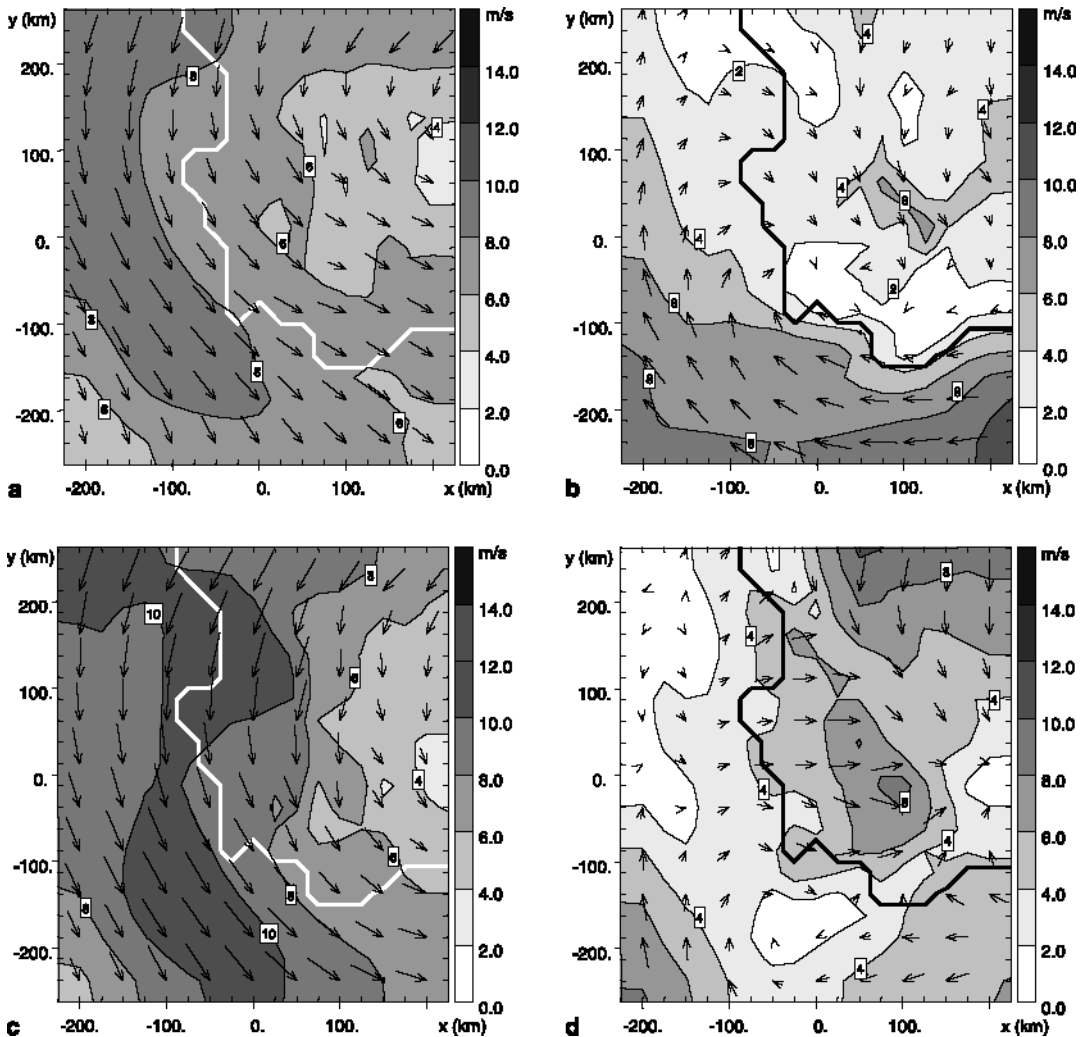


**Fig. 6.** Wind vectors over the extreme South Western Cape (grid 1, 25 km resolution) on 18 February 2000 at 08:00 SAST at **a**)  $z = 2192\text{ m}$ , **b**) surface level ( $z = 24\text{ m}$ ); and at 14:00 SAST at **c**)  $z = 2192\text{ m}$  and **d**) surface level ( $z = 24\text{ m}$ ). Length of vector simulates wind velocity. The black/white lines represent the coastline. Distances ( $x$  and  $y$ ) from the centre grid



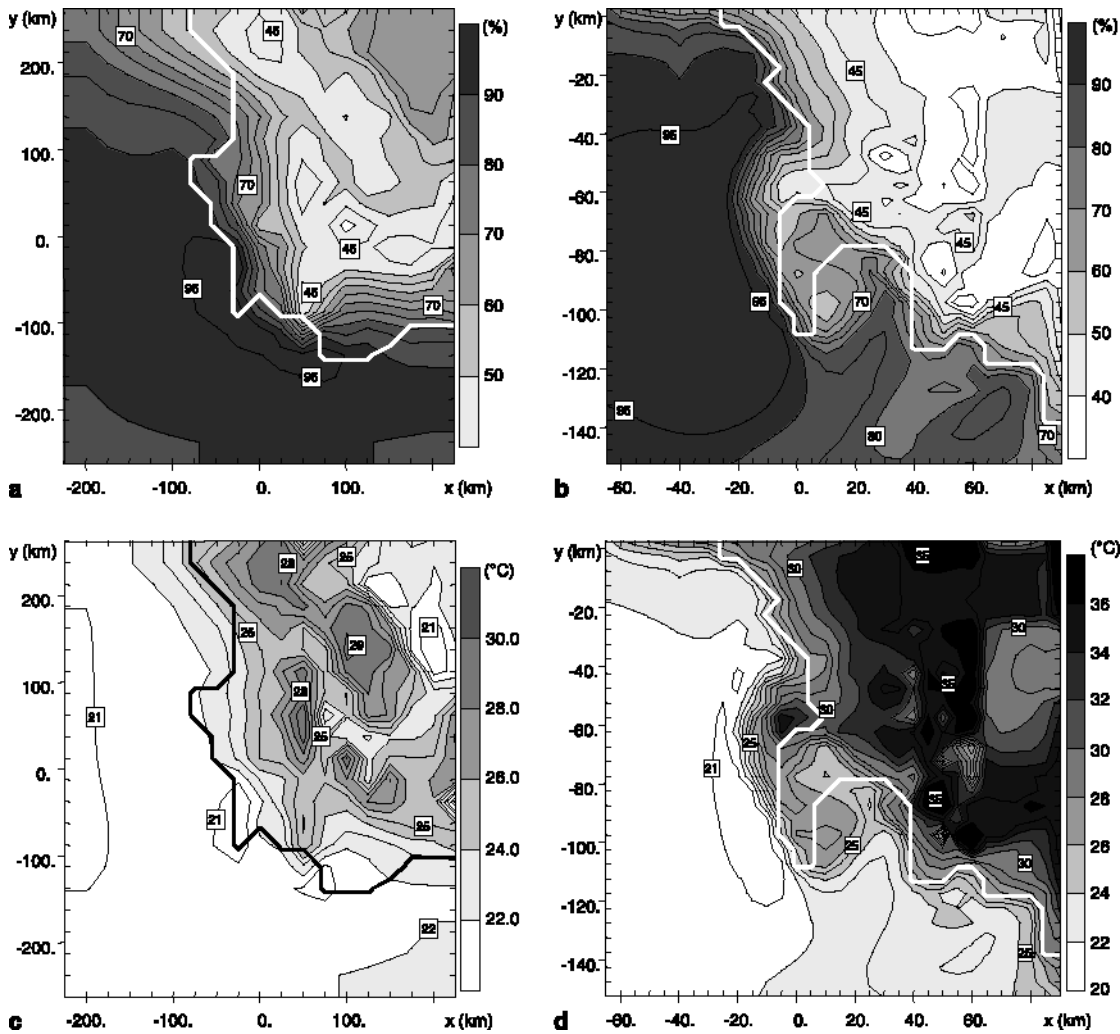


Fig. 7. Relative Humidity (%) on 18 February 2000 over the extreme South-Western Cape at surface level ( $z = 24$  m) at a) 08:00 SAST for grid 1 and b) 14:00 SAST for grid 2 (the white lines represent the coastline); Temperature ( $^{\circ}\text{C}$ ) on 18 February 2000 at surface level ( $z = 24$  m) at c) 08:00 SAST for grid 1 and d) 14:00 SAST for grid 2 (the white and black lines represent the coastline). Distances ( $x$  and  $y$ ) from the centre of grid 1

situated over the interior and the Indian Ocean. At the surface level, a weak northerly wind (Fig. 6b) as well as dry and hot conditions prevailed over the continent (Fig. 7a, c). At 14:00 SAST, the modelled upper wind direction is northerly over the entire domain and the velocity is strengthened (Fig. 6c) compared to the 08:00 SAST winds. The reason for strengthened winds during the day could be an increased vertical mixing during the day, which is observed quite frequently away from mesoscale thermally driven circulations (diurnal cycle of wind speed). The surface wind direction over the continent is still northerly to the north of the domain, with the exception of the northern Atlantic coastal fringe

(Fig. 6d). The deviation of the upper wind (north to northeast) and the strengthening of its velocity above the north western coast (Fig. 6c) may be connected to the return current of a sea breeze blowing from the Atlantic Ocean. The westerly/north-westerly wind to the south of the domain over the extreme South-Western Cape is probably due to the presence of the coastal low developing along the coast and moving south, south-east. The surface wind velocity over the continent is also much stronger than at 08:00 SAST, up to  $8 \text{ m s}^{-1}$  (Fig. 6d). Modelled surface conditions also became drier and hotter (Fig. 7b, d). These patterns are similar to the observations recorded at Cape Town International Airport.

*Fine scale:* At 08:00 SAST, the large-scale flow over the entire domain covered by Grid 3 (1 km resolution) is north-westerly – i.e. onshore for Table Bay and offshore for False Bay – with a velocity between 6 and 8  $\text{m s}^{-1}$  (Fig. 8a), while

the surface wind is predominantly from the north, and weak (Fig. 8b), as observed in the vineyards (Fig. 5a, b), simulating the land breeze. To the south, the land breeze combines with the large-scale wind, and no return current is noticeable

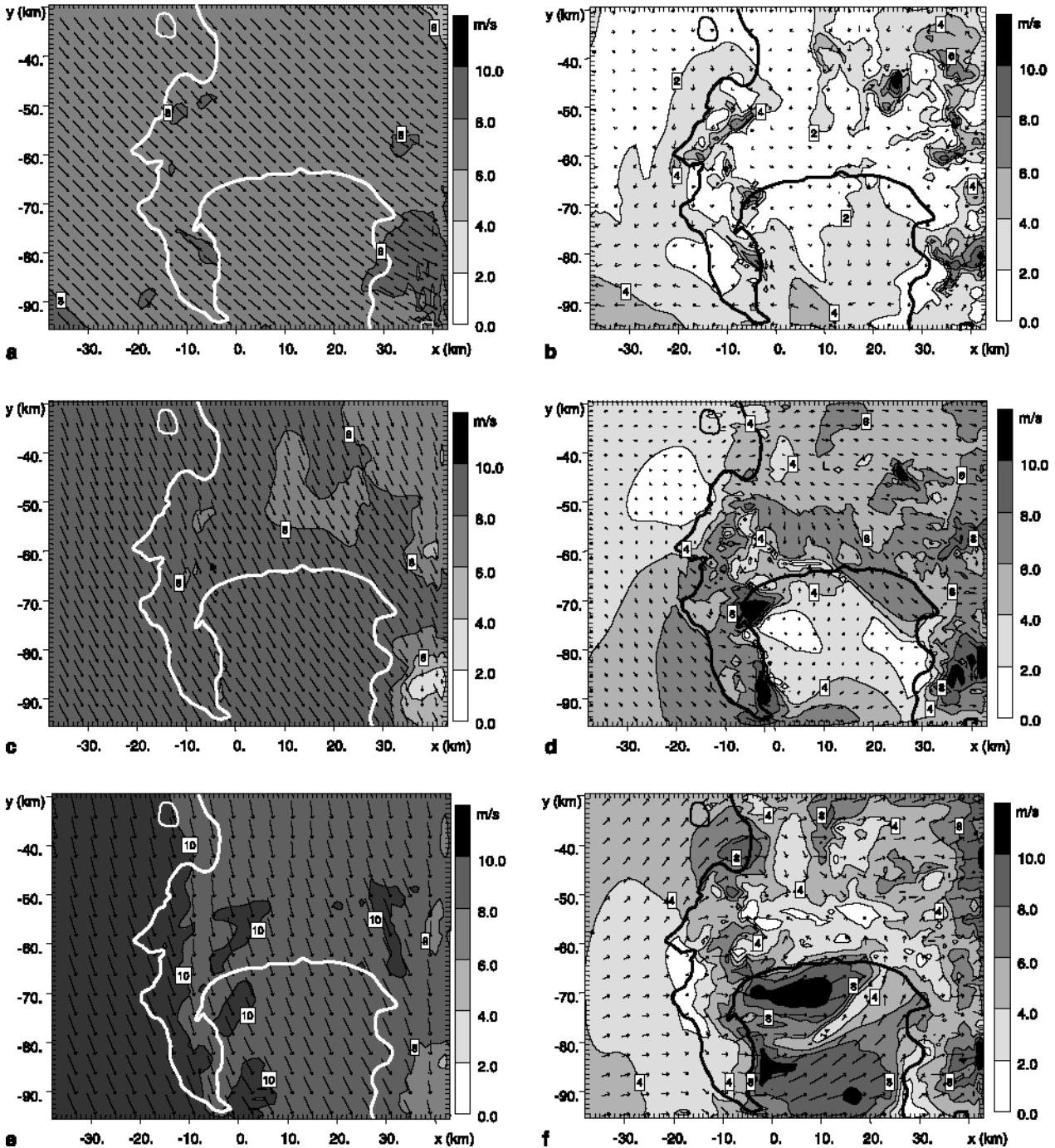


**Fig. 8.** Horizontal wind vectors over the extreme South-Western Cape on 18 February 2000 at  $z = 2192$  m (left) and surface level  $z = 24$  m (right) at 08:00 SAST (a, b); 14:00 SAST (c, d) and 17:00 SAST (e, f). Length of vector simulates wind velocity. The white and black line represents the coastline. Distances ( $x$  and  $y$ ) from the centre of grid 1

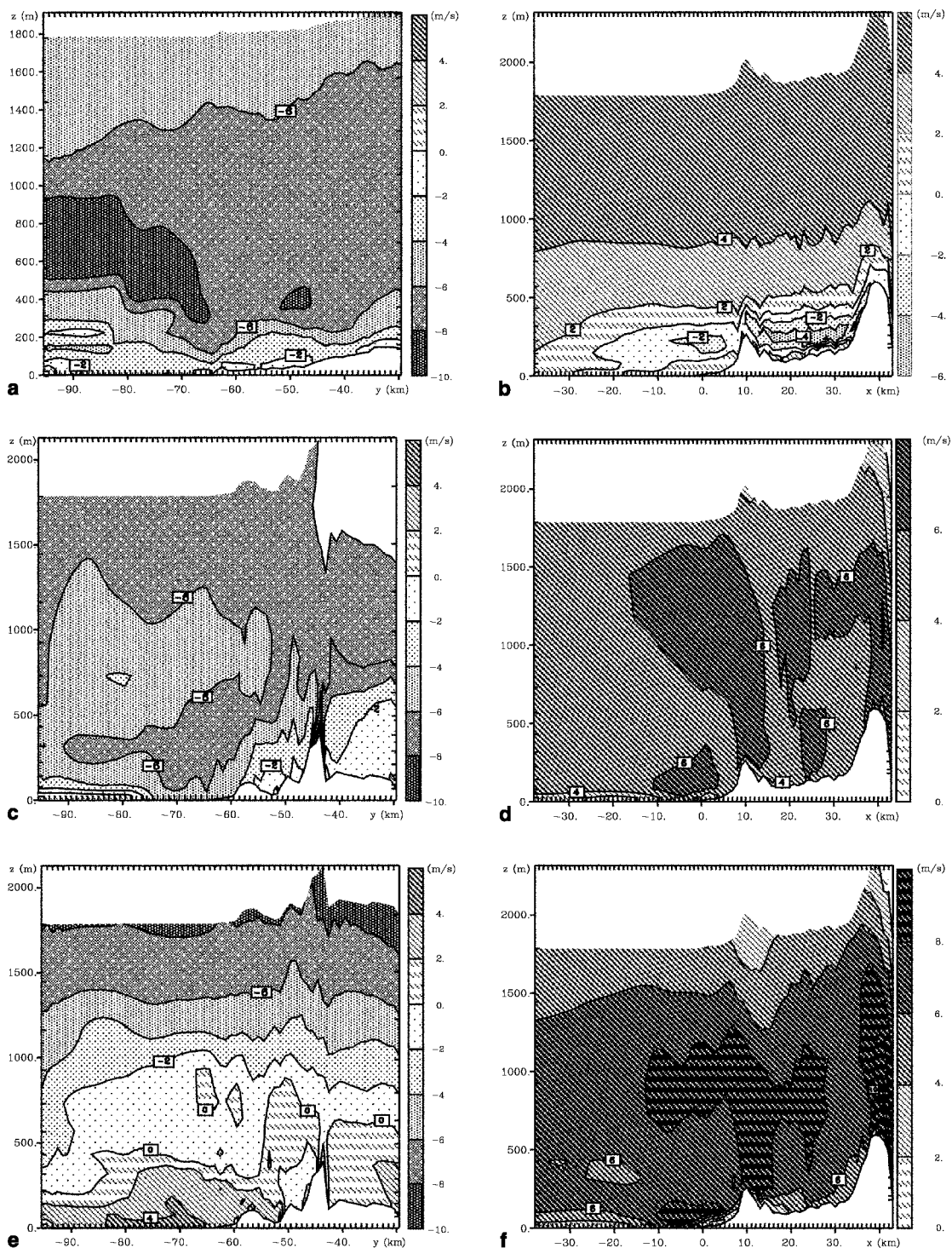


**Fig. 9.** *v* (left) and *u* (right) component of the wind on 18 February 2000 at 08:00 SAST at **a**) 18°41'E ( $X_1$ ) and **b**) 33°47'S ( $Y_1$ ); at 14:00 SAST **c**) 18°47'E ( $X_2$ ) and **d**)  $Y_1$ ; and at 17:00 SAST at **e**)  $X_2$  and **f**)  $Y_1$  over the Stellenbosch wine-producing area. Distances (*x* and *y*) from the centre of grid 1

(Fig. 9a). To the west, the land breeze is 400–500 m deep, flows up to 30 km out to sea with a maximum velocity of at least  $4 \text{ m s}^{-1}$  when combining with the down-slope breeze at the foot of

Simonsberg. The return current combines with the large-scale circulation (Fig. 9b).

At 14:00 SAST, the north-westerly upper wind strengthens to a velocity of  $8 \text{ m s}^{-1}$  (Fig. 8c).

At the surface level, a sea breeze with an Atlantic origin penetrates inland westwards to the north of the study area and turns south/south-eastwards in the direction of False Bay (Fig. 8d), because it combines with the large-scale wind (Fig. 9d), in agreement with the northerly 1000 hPa wind recorded over Cape Town International Airport (Fig. 4b). At the same time, a shallow sea breeze originates over False Bay and opposes the relatively strong northerly synoptic wind (between 6 and 8  $\text{m s}^{-1}$  at 1000 m) and remains out at sea (Fig. 9c). The sea breeze cell circulation over False Bay is less than 500 m deep (return flow included). The sea breeze flow in a strict sense is confined below 100 m with a weak wind velocity (less than 2  $\text{m s}^{-1}$ ), above

which the opposing northerly prevailing flow persists (Fig. 9c). The velocity of its return flow, strengthened by the northerly flow, is up to at least 6  $\text{m s}^{-1}$  at about 300 m. This case is probably one of the most shallow sea breeze circulations compared to the selection of studies of sea breeze depths and return flow mentioned in Oliphant et al. (2001) and shows the effect of the synoptic wind. The land–sea surface thermal gradient was less steep than over the Table Bay area and the northerly prevailing flow opposed the sea breeze.

Later in the afternoon (17:00 SAST), while the large scale wind is further strengthened ( $> 8 \text{ m s}^{-1}$ ) and shifts to a north-northwest direction (Fig. 8e), the two sea breezes converge inland

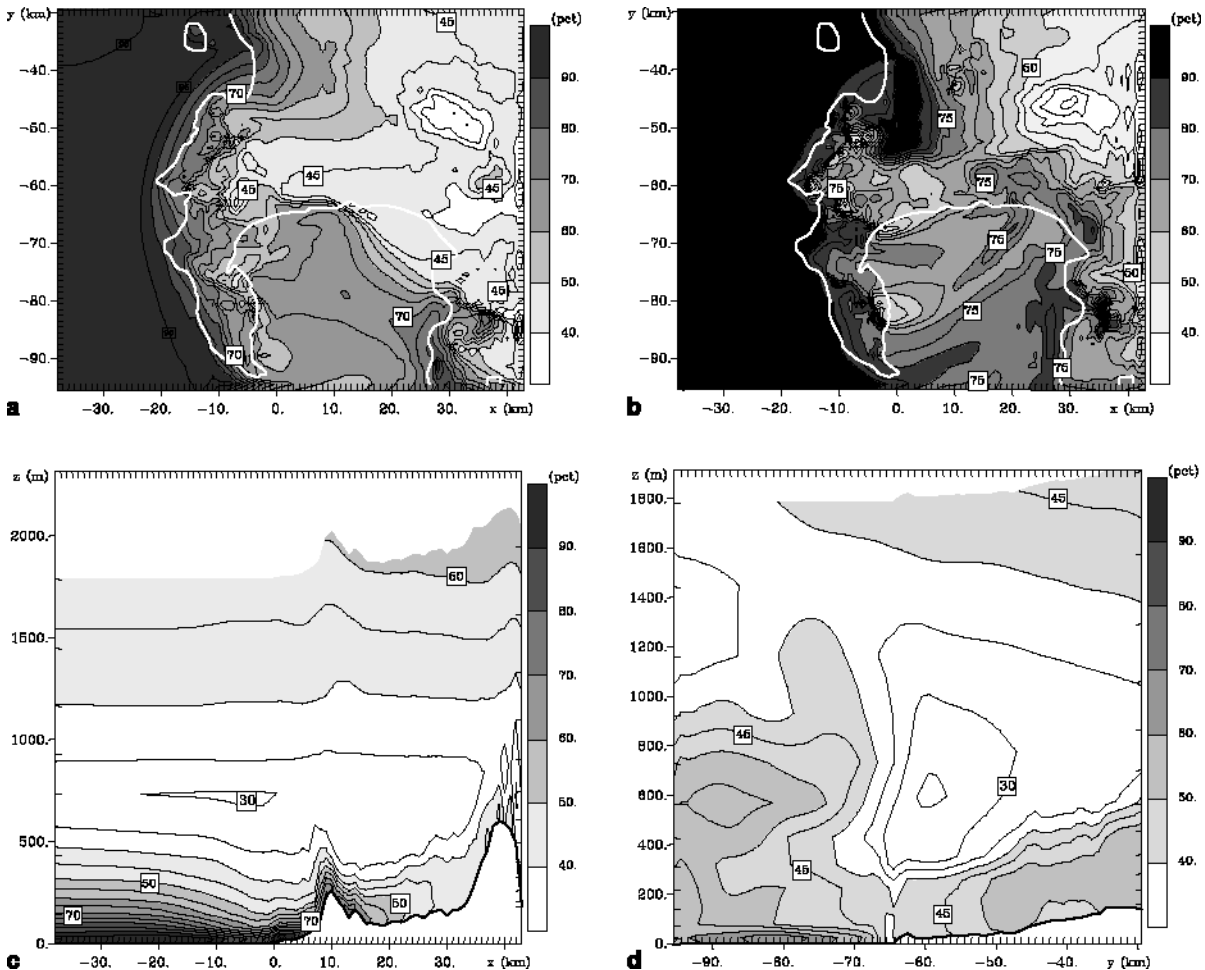


**Fig. 10.** Relative Humidity (%) on 18 February 2000 over the extreme South-Western Cape: at surface level  $z = 24 \text{ m}$  at **a**) 14:00 SAST and **b**) 17:00 SAST (the white line represents the coastline); **c**) West–East cross-section at  $33^{\circ}47'S$  ( $Y_1$ ) and **d**) South–North cross-section at  $18^{\circ}41'E$  ( $X_1$ ) at 14:00 SAST over the Stellenbosch wine-producing area. Distances ( $x$  and  $y$ ) from the centre of grid 1

just over the seaward edge of the wine-producing area at the latitude of CPT and T10 approximately (Fig. 8f). The sea breeze from False Bay thickens (up to 400 m above the bay) and penetrates inland with a maximum wind speed of  $4 \text{ m s}^{-1}$  (Fig. 9e). The return current is deeper (1000 m approximately) and slower (between 2 and  $4 \text{ m s}^{-1}$  at 1000 m) and combines with the large-scale wind at approximately 1500 m.

The two increases in relative humidity observed in the vineyards at 13:00 or 14:00 SAST and 16:00 or 17:00 SAST, depending on the locations (Fig. 5c), resulted from moist air penetration originating from the Atlantic side at 14:00 SAST (Fig. 10a), whereas at 17:00 SAST it resulted from the moist air penetration originating from False Bay (Fig. 10b). At 14:00 SAST, the Atlantic sea breeze, a 400 m thick layer with a relative humidity above 65%, penetrated up

to 15 km eastwards over the Tygerberg hills (Fig. 10c) and reached the wine-producing area on the western slopes of Bottelaryberg, while the moist air from False Bay remained out at sea (Fig. 10d). Simulated values agreed with *observed data* at Cape Town International Airport both at surface and altitude (45–50% vs. 47% at surface and 35% vs. 27% at 12:30 SAST at 1500 m).

The large-scale wind had a significant influence on the formation and landward penetration of the two sea breezes, in similar fashion to observations in other studies (Estoque, 1961, 1962; Savijärvi and Alestalo, 1988; Gustavsson et al., 1995). In the literature, the most intense and well-marked sea breeze fronts were associated with a weak synoptic wind blowing from the opposite direction (Estoque, 1962; Arritt, 1993). However, many studies, cited by e.g.

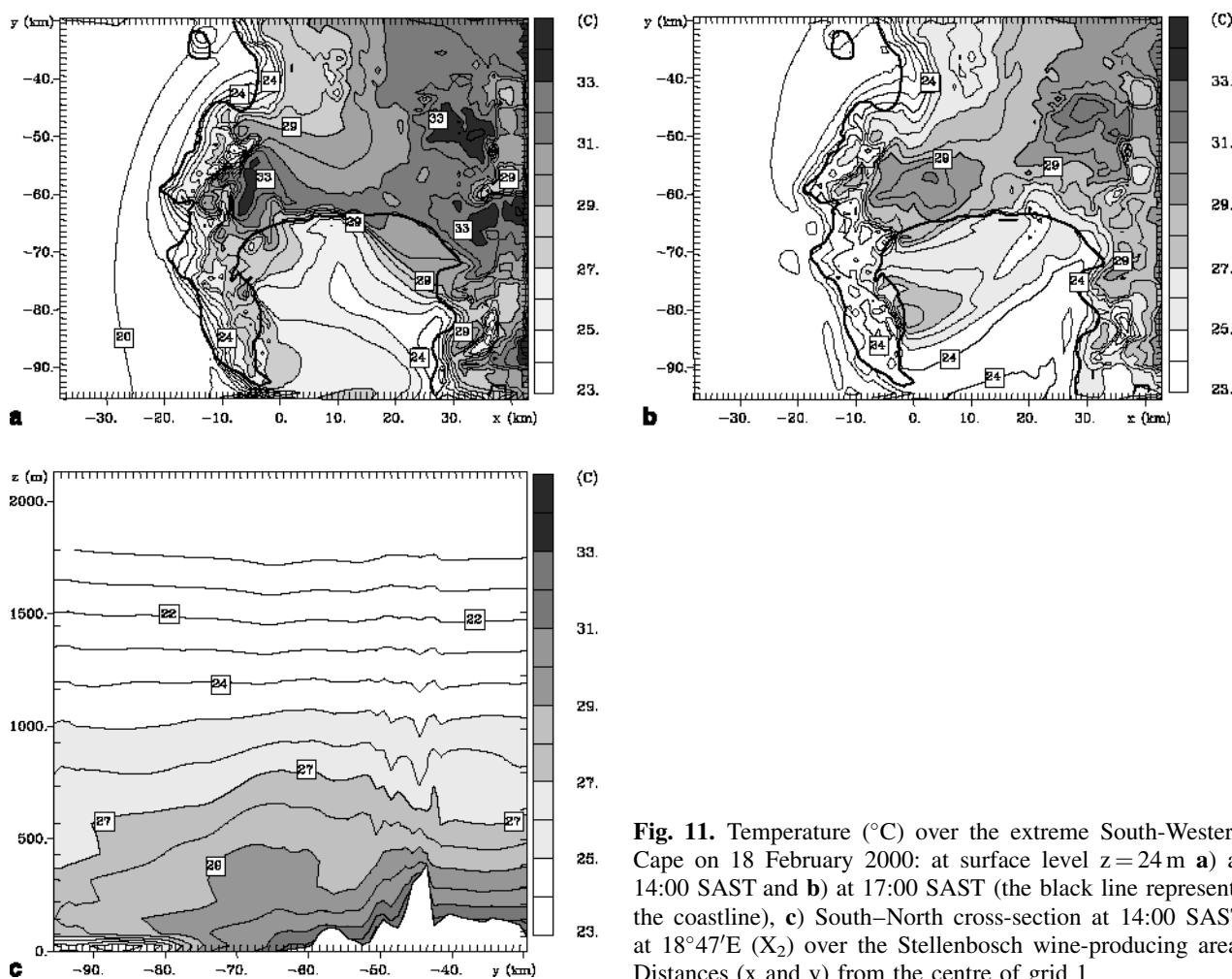


**Fig. 11.** Temperature ( $^{\circ}\text{C}$ ) over the extreme South-Western Cape on 18 February 2000: at surface level  $z = 24 \text{ m}$  **a**) at 14:00 SAST and **b**) at 17:00 SAST (the black line represents the coastline), **c**) South–North cross-section at 14:00 SAST at  $18^{\circ}47'\text{E}$  ( $X_2$ ) over the Stellenbosch wine-producing area. Distances ( $x$  and  $y$ ) from the centre of grid 1

Frizzola and Fisher (1963) and confirmed by numerical simulations (Planchon and Cautenet, 1997; Asimakopoulos et al., 1999; Tijm et al., 1999), report that a strong opposing synoptic flow caused the sea breeze to develop later and further out at sea, or prevented or significantly delayed the inland penetration of the sea breeze. According to several studies cited e.g. by Borne et al. (1998), the sea breeze circulation was eliminated by synoptic conditions when the geostrophic wind exceeded  $6$  or  $8 \text{ m s}^{-1}$ , especially when cool oceanic air advection moved inland, reducing the temperature and surface pressure gradients. In southern France, an offshore wind of more than  $6 \text{ m s}^{-1}$  prevented sea breeze development (Rey, 1967). The present numerical simulations showed that the large-scale wind ( $> 8 \text{ m s}^{-1}$ ), onshore for Table Bay and offshore for False Bay, deflected the sea breeze originating from the Atlantic southwards and stopped the sea breeze developing over False Bay out at sea, the latter reaching the coast at least three hours later (at 17:00 SAST) than with an onshore synoptic flow (Bonnardot et al., 2002), in accordance with the surface data recorded in the vineyards and the upper air data from Cape Town. The sea breeze depth of about 400 m and the wind velocity associated with the simulated sea breeze circulation (return current included) were in accordance with other simulations and observations in warm-temperate areas: in southern Australia (Abbs, 1986; Finkele, 1998), in California (Ulrickson and Mass, 1990) and in north eastern Spain (Massons et al., 1997).

Temperature mainly increases with distance from Table Bay at 14:00 SAST (Fig. 11a), as experienced in the vineyards, with the eastern part of the study domain being the warmest. The west–east temperature gradient prevails over the wine-producing area and provides a cooling effect coming from the Atlantic. The cooling effect over the southern part of the wine-producing area is strengthened during the afternoon with the arrival of the cool air developing over False Bay (Fig. 11b). At 17:00 SAST, the temperature continues to increase with distance from Table Bay, but also from False Bay. Simulated temperature at 14:00 SAST (between  $31$  and  $32^\circ\text{C}$  in the vicinity of T10, and between  $33$  and  $34^\circ\text{C}$  in the vicinity of T15) agrees with

observed surface data in the vineyards ( $31.6^\circ\text{C}$  at T10 and  $34.8^\circ\text{C}$  at T15), whereas a temperature of  $22^\circ\text{C}$  at an altitude of 1500 m (Fig. 11c) agrees with  $24.2^\circ\text{C}$  recorded at 1497 m (850 hPa) over Cape Town at 12:38 SAST.

#### 4. Conclusions

Although the study is based on simulations for one day and thus not necessarily representative of all aspects of “Berg wind” conditions (off-shore airflow) over the Cape, these results complement previous sea breeze investigations over the extreme South-Western Cape with an application to viticulture. The results present the effect of the large-scale flow on the development of two sea breezes, an earlier one developing first from the Atlantic and Table Bay under onshore conditions, and the other developing later from False Bay under offshore conditions, and their convergence over the Stellenbosch wine-producing region. The effect of the sea breeze on temperature, relative humidity and wind was studied. The associated increase in wind velocity may have a negative impact on grapevine functioning, but the temperature reduction, amounting at some locations to as much as  $6^\circ\text{C}$ , reduced the duration and the intensity of the thermal stress experienced by the grapevines under the warm conditions. Further modelling investigations over the wine-producing area using a 200 m grid resolution are in progress in order to assess the local circulations in greater detail.

#### Acknowledgements

The authors express their thanks to the Wine Industry Network of Expertise and Technology (Winetech) and the Centre National de la Recherche Scientifique (CNRS) for funding the research; CINES (Centre Informatique National de l'Enseignement Supérieur), project amp2107 for providing the computer resources; Prof. G Cautenet, AM Lanquette and F Besserve (LaMP) and I Ganzetti (COSTEL) for technical assistance; VA Carey (Stellenbosch University, project leader of the WW13/02 ARC Infruitec-Nietvoorbij project under which the present research falls) for the viticultural input; the ARC-Institute for Soil, Climate and Water, the ARC-Infruitec/Nietvoorbij Institute, the South African Weather Service, the National Oceanic and Atmospheric Administration and the European Centre for Medium Range Weather Forecast for providing the different data sets required for the study and the reviewers for their valuable comments.

## References

- Abbs DJ (1986) Sea breeze interactions along a concave coastline in Southern Australia: observations and numerical modelling study. *Mon Wea Rev* 114(5): 831–848
- Abbs DJ, Physick WL (1992) Sea breeze observations and modelling: a review. *Aust Met Mag* 41: 7–19
- Arritt RW (1993) Effects of the large-scale flow on characteristic features of the sea breeze. *J Appl Meteorol* 32: 116–125
- Asimakopoulos DN, Helmis CG, Papadopoulos KH, Kalogiros JA, Kassomenos P, Petrakis M (1999) Inland propagation of sea breeze under opposing offshore wind. *Meteorol Atmos Phys* 70: 97–110
- Bonnardot V (1997) Sea breeze effect on temperature in the Stellenbosch-Klein Drakenstein wine-producing district in South Africa. Internal Research Report (WW13/02 project), ARC-Infruited/Nietvoorbij Institute, Stellenbosch, RSA. 42p + Figures (unpublished data)
- Bonnardot V (1999) Étude préliminaire des brises de mer pendant la période de maturation dans la région viticole du Cap en Afrique du Sud. *Pub Assoc Int Climatol* 12: 26–33
- Bonnardot V, Carey VA, Planchon O, Cautenet S (2001) Sea breeze mechanism and observations of its effects in the Stellenbosch wine producing area. *Wynboer* 147: 10–14. (In South African Wineland magazine, October 2001)
- Bonnardot V, Planchon O, Carey VA, Cautenet S (2002) Diurnal wind, relative humidity and temperature variation in the Stellenbosch-Groot Drakenstein wine producing area. *S Afr J Enol Vitic* 23(2): 62–71
- Borne K, Chen D, Nunez M (1998) A method for finding sea breeze days under stable synoptic conditions and its application to the Swedish west coast. *Int J Climatol* 18: 901–914
- Campbell-Clause JM (1988) Stomatal response of grapevines to wind. *Austr J Exp Agr* 38: 77–82
- Carey VA, Archer E, Saayman D (2002) Natural terroir units: What are they? How can they help the wine farmer? *Wynboer* 151: 86–88. (In South African Wineland magazine, February 2002)
- Champagnol F (1984) *Eléments de Physiologie de la Vigne et de Viticulture Générale*. François Champagnol, Saint-Gely-du-Fesc (ISBN 2-9500614-0-0), France, 351p
- Clark TL, Farley RD (1984) Severe downslope windstorm calculations in two and three spatial dimensions using anelastic interactive grid nesting: A possible mechanism for gustiness. *J Atmos Sci* 41: 329–350
- Coombe BG (1987) Influence of temperature on composition and quality of grapes. *Acta Hort* 206: 23–33
- Cotton WR, Pielke Sr RA, Walko RL, Liston GE, Tremback CJ, Jiang H, McAnely RL, Harrington JY, Nicholls ME, Carrio GG, McFadden JP (2003) *Rams 2001: Current status and future directions*. *Meteorol Atmos Phys* 82: 5–29
- Düring H (1976) Studies on the environmentally controlled stomatal transpiration in grape vines. I Effects of light intensity and air humidity. *Vitis* 15(2): 82–87
- Estoque MA (1961) A theoretical investigation of the sea breeze. *Quart J Roy Meteor Soc* 82: 136–146
- Estoque MA (1962) The sea breeze as a function of the prevailing synoptic situation. *J Atmos Sci* 19: 244–250
- Finkele K (1998) Inland offshore propagation speeds of a sea breeze from simulations and measurements. *Bound-Layer Meteor* 87: 307–329
- Freeman BM, Kliever WM, Stern P (1982) Research note. Influence of windbreaks and climatic region on diurnal fluctuation of leaf water potential, stomatal conductance, and leaf temperature of grapevines. *Am J Enol Vitic* 33(4): 233–236
- Frizzola JA, Fisher EL (1963) A series of sea breeze observations in the New York City area. *J Appl Meteor* 2: 722–739
- Gladstones J (1992) *Viticulture and environment*. Winetitles, Adelaide (ISBN 1875130128), 310p
- Gustavsson T, Lindqvist S, Borne K, Bogren J (1995) A study of sea and land breezes in an archipelago on the West Coast of Sweden. *Int J Climatol* 15: 785–800
- Hamilton RP (1989) Wind and its effects on viticulture. *Austr Grapegr Winemaker* pp 16–17
- Huglin P, Schneider C (1998) *Biologie et Écologie de la Vigne*. Lavoisier TEC&DOC, 2<sup>nd</sup> edn. Paris (ISBN 2743002603), 370p
- Jackson SP (1954) Sea breezes in South Africa. *S Afr Geogr J* 36: 13–23
- Janoueix-Yacono D (1995) Rapport entre brise de mer ou de lac, structure de la couche-limite planétaire et pollution atmosphérique sur des plaines littorales urbanisées, In: *Climat, Pollution atmosphérique, Santé – Hommage à Gisèle Escourrou*, Dijon, pp 177–201
- Kliever WM, Torres RE (1972) Effect of controlled day and night temperatures on grape coloration. *Am J Enol Vitic* 23(2): 71–77
- Kriedemann PE (1977) Vine leaf photosynthesis. In: *Proc. Int. Sym. Quality of the Vintage, February 1977, Cape Town, South Africa*, pp 67–88
- Land type survey staff (1995) *Land types of the map 3318 CAPE TOWN*. Mem. Agric. Nat. Resour, S. Afr., 24. Institute for Soil, Climate and Water of the Agricultural Research Council
- Lindesay JA, Tyson PD (1990) Thermo-topographically induced boundary layer oscillations over the Central Namib, Southern Africa. *Int J Climatol* 10: 63–77
- Mahrer Y, Pielke RA (1977) The effects of topography on sea and land breezes in a two-dimensional numerical model. *Mon Wea Rev* 105: 1151–1162
- Maritz L (2001) *Wind and temperature over the Stellenbosch wine producing area*. Research methodology: Meteorology – WKD 713, Department of Earth Science: Meteorology, University of Pretoria, 30p
- Massons J, Camps J, Soler MR (1997) Modeling of pollutant dispersion in sea breeze conditions using a Lagrangian model. *Theor Appl Climatol* 56: 255–266
- Oke TR (1978) *Boundary layer climates*. London: Methuen, 372 p
- Oliphant AJ, Sturman AP, Tapper NJ (2001) The evolution and structure of a tropical island sea/land-breeze system, northern Australia. *Meteorol Atmos Phys* 78: 45–59
- Physick WL, Abbs DJ (1991) Modeling of summertime flow and dispersion in the coastal terrain of southeastern Australia. *Mon Wea Rev* 119: 1014–1030

- Pielke RA, Cotton WR, Walko RL, Tremback CJ, Lyons WA, Grasso LD, Nicholls ME, Moran MD, Wesley DA, Lee TJ, Copeland JH (1992) A comprehensive Meteorological Modeling System – RAMS. *Meteorol Atmos Phys* 49: 69–91
- Planchon O, Cautenet S (1997) Rainfall and sea breeze circulation over southwestern France. *Int J Climatol* 17(5): 535–549
- Planchon O, Bonnardot V, Cautenet S (2000) Simulation de brise de mer dans la Province Occidentale du Cap (Résolution à 5 km): Exemple de la journée du 4 février 2000. *Pub Assoc Int Climatol* 13: 482–489
- Preston-Whyte RA (1969) Sea breeze studies in Natal. *S Afr Geogr J* 51: 38–49
- Rey P (1967) Etude biogéographique du vent sur le littoral Languedoc-Roussillon. Service de la carte de la végétation, CNRS, Fasc II, 143 + 86 p
- Savijärvi H, Alestalo M (1988) The sea breeze over a lake or gulf as the function of the prevailing flow. *Beitr Phys Atmos* 61: 98–104
- South African Weather Service (SAWS) (2000) Daily weather bulletin (February 2000), Pretoria: Department of Environmental Affairs and Tourism
- Tijm ABC, Van Delden AJ, Holtslag AAM (1999) The inland penetration of sea breezes. *Contrib Atmos Phys* 72(4): 317–332
- Tyson PD, Seely MK (1980) Local winds over the central Namib. *S Afr Geogr J* 62: 135–150
- Ulrickson BL, Mass CF (1990) Numerical investigation of mesoscale circulations over the Los Angeles basin. Part I: A verification study. *Mon Wea Rev* 118(10): 2138–2161
- Walko RL, Tremback CJ, Pielke RA, Cotton WR (1995) An interactive nesting algorithm for stretched grids and variable nesting ratios. *J Appl Meteor* 34: 994–999
- White ID, Mottershead DN, Harrison SJ (1992) *Environmental systems: an introductory text*, 2nd edn. London: Chapman & Hall (ISBN 041247140X) 616 p

Authors' addresses: Dr. Valérie Bonnardot (e-mail: Valerie@infruit.agric.za), ARC-ISCW, Private Bag X5026, Stellenbosch 7599, South Africa; Dr. Olivier Planchon (e-mail: Olivier.planchon@uhb.fr), COSTEL, University of Rennes-2, Place Recteur H. Le Moal, CS 24 307, 35043 Rennes-Cedex, France; Prof. Sylvie Cautenet (e-mail: s.cautenet@opgc.univ-bpclermont.fr), LaMP, Blaise Pascal University, 24 Avenue des Landais, 63177 Aubière, France.